

# Aerosol optical properties over marine and continental sites of India during pre-monsoon season

Piyush Patel\* and A. K. Shukla

Calibration and Validation Division, Space Applications Centre, Indian Space Research Organisation, Ahmedabad 380 015, India

**Ground and satellite based measurements of spectral optical properties of aerosols have been carried out at Dehradun (DDN) in the Indo-Gangetic Plain (IGP) and Kavaratti (KVT) at Lakshadweep in southern Arabian Sea during pre-monsoon season (March–May) 2012. The measurements illustrate distinct seasonal impact on aerosol properties with maximum dust loading during May in conjunction with anthropogenic aerosols over DDN and marine aerosols over KVT. Aerosol optical depth (AOD) values have been observed maximum in May ( $0.72 \pm 0.03$ ) over DDN and in April ( $0.77 \pm 0.05$ ) over KVT. The high AOD at DDN during May is associated with low  $\alpha$  and high  $\beta$ , means higher loading in May is associated with coarse mode aerosols, may be dust loading as evident from SSA and volume size distribution. Similarly, high AOD at KVT during March and April are associated with high  $\alpha$  and low  $\beta$ , may be due to anthropogenic influence as evident from BT analysis as well as SSA and volume size distribution. However, influence of marine aerosols is also noticeable over KVT during May as indicated by the lower values of  $\alpha$  with high turbidity coefficient  $\beta$ . Comparison between sunphotometer and MODIS AOD observations indicates good statistical agreement with the minimal error.**

**Keywords:** Angstrom exponent, AOD, MODIS, single scattering albedo.

ATMOSPHERIC aerosol plays an important role by interacting with radiation and modifying cloud microphysical properties, although the magnitude of these events remain uncertain in regional and global climate<sup>1</sup>. Large spatio-temporal variability of aerosols leads to change in atmospheric heating<sup>2–4</sup>. Both scattering and absorption of radiation involved in the direct interaction of aerosols, and the relative importance of these processes depend on their chemical composition, size distribution and refractive index. The chemical and physical properties of aerosols are strongly dependent on their sources. The aerosol sources are highly variable and differ on a regional basis leading to variation in the Earth's radiation budget. Moreover, transportation of aerosols from one place to another

has a different kind of impact, which has to be studied for both over ocean as well as land. Studies of aerosols over oceans are important from the standpoint of understanding anthropogenic and continental impacts over oceans as well as in estimations of aerosol radiative forcing<sup>5,6</sup>.

The study focuses on variability of aerosols and its properties over continental as well as marine sites of India during the pre-monsoon period (March–May 2012). Two sites were selected with distinct weather and climate differences. One of them is Dehradun (DDN), pure continental site, along with mixing of anthropogenic, dust and biomass burning aerosols. The other site is Kavaratti (KVT), Lakshadweep, pure marine site with the dominance of marine aerosols, for e.g. sea-salt mixing with continental aerosols and soil-dust transported from continental land. Variability of the aerosols over different regions has different impacts on local climate. From INDOEX observations, Satheesh and Ramanathan<sup>7</sup> suggested that the large aerosol surface forcing over the Indian Ocean region can influence the hydrological cycle in the tropics and has a far reaching impact on weather. Vinoj and Satheesh<sup>8</sup> made aerosol optical measurements during the summer monsoon and showed enhanced aerosol load over the northern Arabian Sea region. They attributed this large aerosol loading to the sea-salt aerosol generated due to high winds over the Arabian Sea. Similarly over land, the most striking feature of the IGP is that mineral dust adds to the anthropogenic pollution load in the pre-monsoon and monsoon seasons<sup>9,10</sup>. Previous studies over the IGB showed distinct seasonal patterns of aerosol properties controlled by the northeast and summer monsoon<sup>11–14</sup>. There seems to be insufficient knowledge on aerosol variability over the Kavaratti, Lakshadweep and Dehradun, Uttarakhand region, especially during pre-monsoon season (March to May), which is presented in this study.

## Study areas and meteorological conditions

### *Dehradun, Uttarakhand*

Dehradun (30°30'N and 78°36'E) is the capital of Uttarakhand state as well as the district headquarters (Figure 1). It is located in the Shivalik range of the Himalayas at a

\*For correspondence. (e-mail: piyushastrophy@gmail.com)

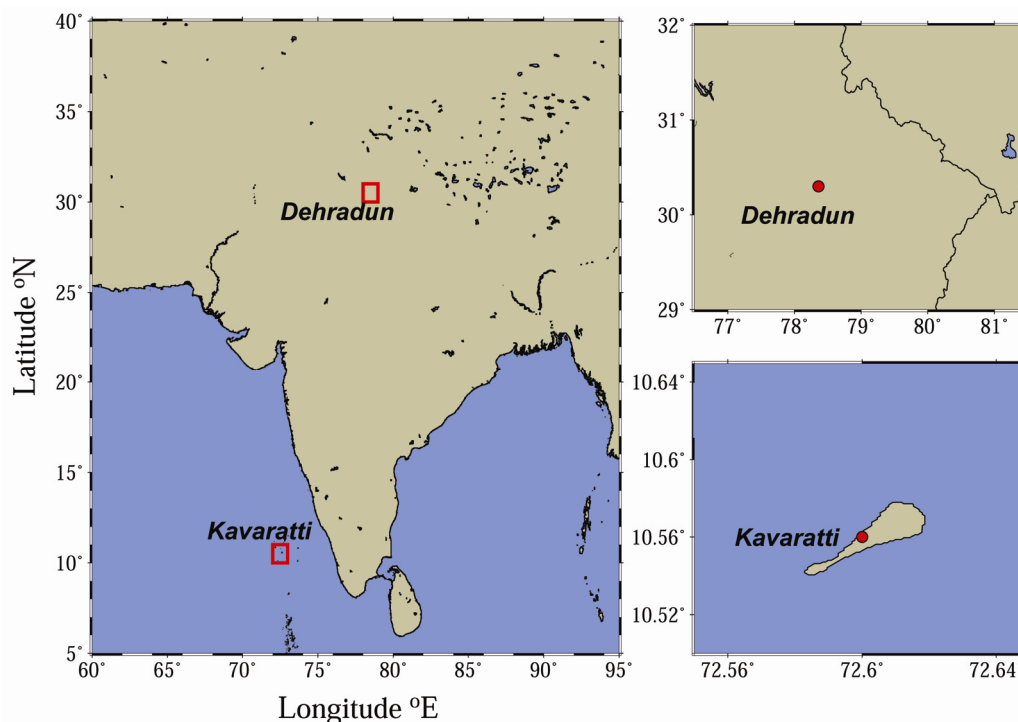


**Figure 1.** Study areas. (1) Dehradun, Uttarakhand and (2) Kavaratti, Lakshadweep.

mean altitude of 700 m amsl, extends 80 km in length and ~20 km in average width. Dehradun is located in a valley surrounded by hills. This region experiences four dominant seasons each year, namely, winter (December–February), pre-monsoon (March–May), monsoon (June–September) and post-monsoon (October–November). During pre-monsoon season, air mass carries dust particles by southwesterly winds from Thar Desert<sup>15</sup>, and during post-monsoon season, atmosphere is loaded with black carbon and other fine mode organic particles due to large-scale biomass burning from the Indo-Gangetic plain. In addition to this, the region is influenced by urban pollution, mining activities (mainly limestone), and forest fires<sup>16</sup>.

The climate of Dehradun is generally temperate and varies from being hot in summers to severely cold in winter, depending upon the season. The nearby hilly regions often receive snowfall during winter but the temperature in Dehradun is not known to decrease below freezing values. Summer temperatures can often reach 40°C; whereas, winter temperatures are usually between 2°C and 20°C. The mean annual rainfall is ~2200 mm. Significant amount of rainfall occurs from June to September, which accounts for 70–80% of the total annual rainfall. The relative humidity is generally less than 55% during summer, around 60–65% during winter and 80–85% during monsoon.

#### *Kavaratti, Lakshadweep*

Kavaratti (10°56'N and 72°6'E) Island is the capital of the Union Territory of Lakshadweep (Figure 1). Area of

the island is 4.22 sq. km; maximum length is 5.8 km and width is 1.6 km. It has a lagoon having a length of about 6 km and an area of 4.96 sq. km. The island is 2–5 m amsl on the western side and 2–3 m on the eastern side. Kavaratti has a small inland lake at its northern end. The island itself is stretched over an area of slightly more than 4 sq. km and has the maximum percentage of non-islanders as residents.

Climate of Kavaratti is similar to the climatic conditions of Kerala. The temperature ranges from 25°C to 35°C and humidity ranges from 70% to 76% for most of the year. The average rainfall received is 1600 mm a year. Monsoon prevails here from mid-May to mid-September. The monsoon period raises temperature to mercury level between 27°C and 30°C.

#### *Wind patterns*

Monthly variation of average wind pattern at 850 mb over India and over Arabian Sea is described in Figure 2 using NCEP reanalysis datasets. Wind speed is generally low and less than 4.0 m s<sup>-1</sup> and found to increase more in May than March and April over DDN. Wind direction is predominantly from westerly to north westerly (Arabian countries) during pre-monsoon (March–May), which is responsible for dust transportation over Dehradun from the desert region.

Wind pattern over the island is largely seasonal, with north-westerlies/westerlies during April to October, changing to north-easterlies/easterlies for the rest of the

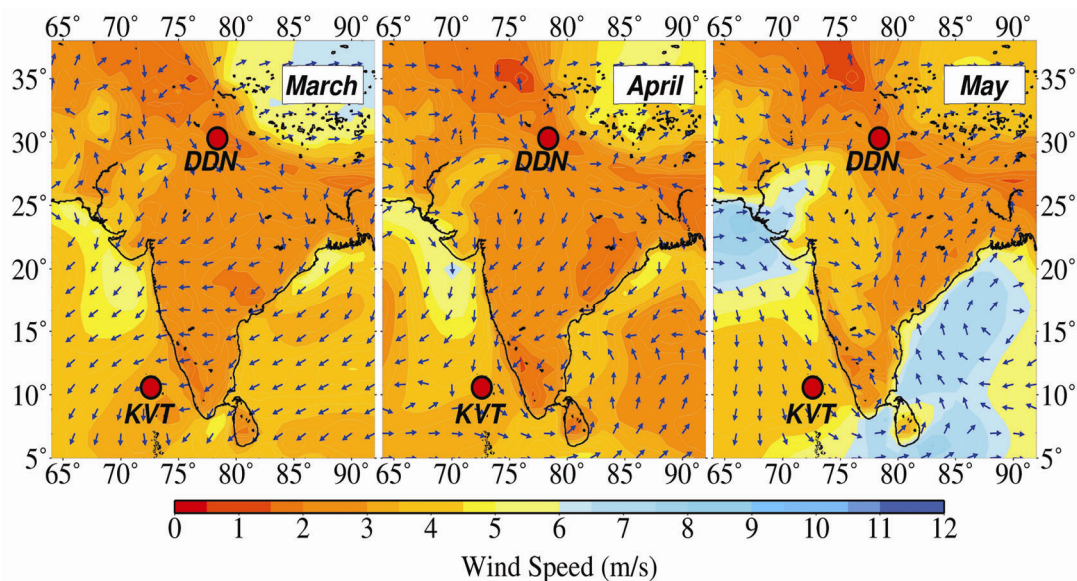


**Figure 2.** Wind pattern over India during pre-monsoon season along with the location of study areas, Dehradun and Kavaratti.

year. March is characterized by winds mostly from the Indian subcontinent, which is expected to be largely anthropogenic nature. April can be said to be the transition period between pre-monsoon and monsoon. Further, winds from northwest to Arabian Sea might be influenced by dust from the Saudi Arabian desert region during May<sup>17</sup>.

## Datasets and instruments

### Dehradun, Uttarakhand

Aerosol optical depth (AOD) measurements over DDN were made using a multi wavelength Microtops-II sun-photometer (Solar Light Co, USA). It measured AOD of five different wavelengths at 380, 440, 500, 675 and 870 nm from the solar instantaneous flux measurements with its internal calibration. An ozone monitor measures the total column ozone at three different UV channels (305.5, 312.5 and 320.0 nm) in Dobson unit (DU) along with water vapour column at two near-IR channels (940 and 1020 nm) in centimetres. It also measures AOD at 1020 nm. Thus, the AOD obtained for six wavelengths from both the sets of MICORTOPS-II are utilized to retrieve the wavelength exponent, which is an index of aerosol size distribution. Simultaneously, continuous measurements of black carbon (BC) were carried out using aethalometer model AE-42 of Magee Scientific, USA. The instrument was operated continuously on a 24 h cycle at a flow rate of 4 l/min at sampling rate of 5 min interval and aspirated ambient air using an inlet tube from ~15 m above the ground. An optical transmission technique was used along with continuous filtration

in an aethalometer to measure the concentration of BC. Similarly, satellite observations were used during this study, for e.g. MODIS.

### Kavaratti, Lakshadweep

A robotic CIMEL sunphotometer was used to measure AOD over KVT. It consists of eight filters whose wavelengths are centred at 340, 380, 440, 500, 670, 870, 936 and 1020 nm and the full width at half maxima (FWHM) is 10 nm. Two collimators with the 1.2° field of view are present in this unit. The CIMEL sun-photometer provides the spectral AOD at eight wavelengths (as given above), Angstrom exponent ( $\alpha$ ) (440–870 nm) and the water vapour content (WVC) at 940 nm using its internal calibration for direct irradiance<sup>18</sup>. Furthermore, the aerosol volume size distribution is retrieved through sun and sky measurements using improved version of Skyrad.pack radiative transfer code (version 4.2) in the range  $0.01 \mu\text{m} \leq \text{particle radius} \leq 8.4 \mu\text{m}$ . The single scattering albedo (SSA) and asymmetry parameter ( $g$ ) are retrieved through a non-spherical aerosol method introduced by Olmo *et al.*<sup>20</sup> in the four different wavelengths. The sunphotometer recordings are performed for clear sky days. The aerosol properties have been averaged on daily basis during this study.

### MODIS AOD data

Moderate resolution imaging spectroradiometer (MODIS) acquires daily global data in 36 bands. MODIS is onboard the polar orbiting NASA Terra and Aqua satellites

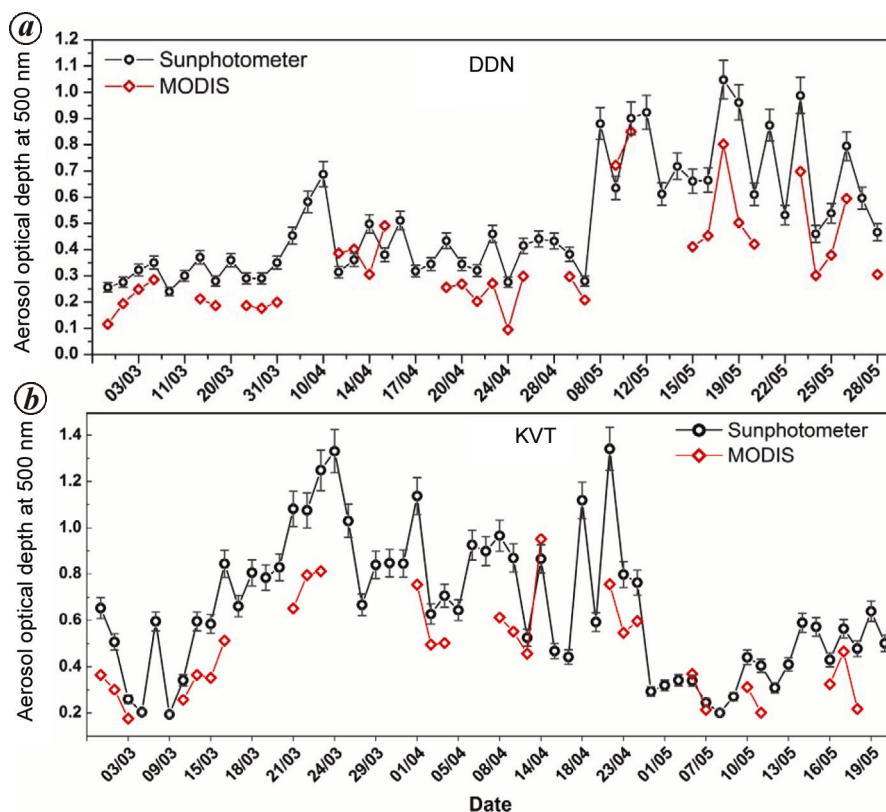


**Figure 3.** Variation of daily averaged AOD measured by sunphotometer and MODIS satellite over (a) DDN and (b) KVT during pre-monsoon seasons (March–May 2012).

with equator crossing time of 10:30 and 13:30 local solar time respectively. Two different algorithms have been used to retrieve the AOD from MODIS data over land and ocean<sup>21</sup>. Inversion of observed reflectance using radiative transfer look-up table based on aerosol models has been used to derive aerosol properties from MODIS<sup>22,23</sup>. MODIS-derived AOD datasets have been analysed for comparison over both continental and marine sites during the study period. Data used in this study include Terra and Aqua MODIS aerosol products, calculated using separate algorithms over land and ocean to obtain AOD at 550 nm ( $AOD_{550}$ ). The C005 Level 3 MODIS products (spatial resolution  $1^\circ \times 1^\circ$ ) were obtained from LADSWEB website (<http://ladsweb.nascom.nasa.gov/>).

## Results and discussion

### *Aerosol optical properties*

AOD indicates the aerosol burden in the local atmosphere. AOD at 500 nm is considered as the representative of the entire AOD spectra closest to the central part of the whole spectral range. Figure 3 describes the daily variation of AOD at 500 nm over both the sites during pre-monsoon season. The result reveals significant day-

to-day variability in AOD, which indicates the impact of the local meteorology, variety of aerosol types and sources. Here, both sites have different kinds of AOD variations during pre-monsoon, which may be due to the different types and sources of aerosol and differences in local climate. The AOD variation is found to be almost similar during March ( $0.30 \pm 0.04$ ) and April ( $0.43 \pm 0.08$ ) over DDN but sudden increment of AOD is observed in May ( $0.79 \pm 0.09$ ), which suggests an extra loading of total columnar aerosol in the atmosphere. This extra loading may be due to air mass transportation, which has been analysed through seven-day isentropic back trajectories over the region. Figure 4 describes the analysis of seven-day isentropic back trajectories at 2000 m above ground level along with distribution of relative humidity for all days over both the sites.

Analyses of trajectories over DDN indicate that the air masses come from arid locations in north-western and western (Thar Desert) region, which carry dust aerosols from arid region along with anthropogenic aerosols from polluted cities located (Delhi, Punjab, etc.) in the western side of the study location. This leads to enhanced aerosol loading in the local atmosphere.

AOD variation over KVT is quite different from DDN. Average value of AOD over KVT ( $0.64 \pm 0.13$ ) is found to be higher than over DDN ( $0.51 \pm 0.10$ ), which may be

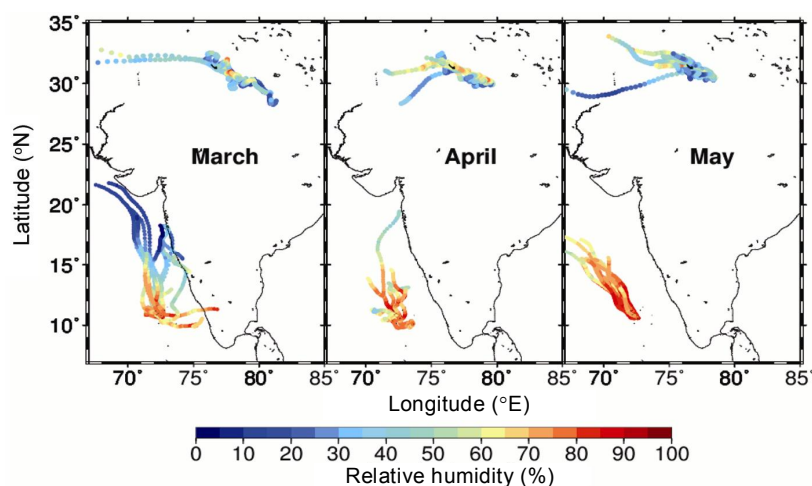


**Figure 4.** Seven days back trajectory analysis over both the sites during pre-monsoon seasons.

due to all-time presence of marine aerosol (e.g. sea-salt) over KVT. Larger value of AOD has been observed in March ( $0.73 \pm 0.13$ ) and April ( $0.77 \pm 0.16$ ) over KVT than May ( $0.45 \pm 0.09$ ). Analysis of air-mass back trajectories (Figure 4) indicates that polluted air mass along with continental aerosols are transported from the north-eastern direction (the Indian mainland) during March and April and it shifts in north-western direction (Arabian countries) during May, which carries dust aerosols along with marine aerosols. Large transportation of continental aerosols leads to increase in AOD during March and April over KVT. Simultaneous to analysis with sunphotometer, the MODIS aerosol product has been analysed to study the variation of AOD over both the sites. The result reveals the almost similar variation of MODIS-derived AOD over both sites which are shown in Figure 3. MODIS-evaluated aerosol loading is lower than that of sunphotometer. MODIS-derived AOD is found to be more similar to sunphotometer over marine site than over continental site. This may be due to the retrieval, which is easier over ocean than over land. Further, spectral variation of AOD has been analysed for the study of particle size variation.

Figure 5 describes monthly variation of spectral AOD for both the sites. Transportation of aerosols from western region leads to the gradual increment in AOD from March to May over DDN. The increment in AOD has been detected more in longer wavelength compared to shorter wavelength suggesting the dominance of coarse mode particles during transportation. The mean AOD value ( $0.51 \pm 0.18$ ) during pre-monsoon is observed over DDN, which is higher than other cities that are not so industrialized<sup>24,25</sup>. The AOD spectrum illustrates a peak during May at longer wavelengths, suggesting a dominance of coarse (dust) particles and weak dependency of AOD over DDN. However, the presence of dust particle increases AOD in both shorter and longer wavelengths due to enhancement in interaction of the solar radiation at the longer wavelength<sup>26</sup>.

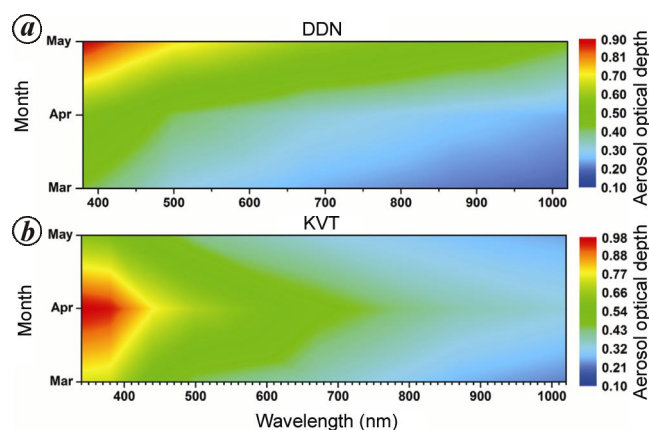


**Figure 5.** Spectral variation of AOD over (a) DDN and (b) KVT during pre-monsoon.

In KVT, significant higher spectral AOD values appear during March–April and decrease towards May, while the peak was strong in March and April. High variation of AOD has been observed at shorter wavelength than longer wavelength. Variation of AOD at longer wavelength is found to be smaller (0.30–0.35) than over DDN (0.20–0.50). This indicates the loading of fine mode aerosols over KVT during March and April because fine mode particles increase AOD only at shorter wavelength. The averaged AOD value ( $0.64 \pm 0.20$ ) observed during pre-monsoon indicates large amount of continental aerosol transport along with air mass from Indian mainland to KVT. For further investigation, Angstrom exponent and turbidity coefficient have been studied.

Variation of Angstrom exponent ( $\alpha$ ) and turbidity coefficient ( $\beta$ ) are shown in Figure 6. Angstrom exponent is an important aerosol parameter for the study of aerosol size distribution in the local atmosphere. Lower value of  $\alpha$  indicates dominance of coarse mode particles (or lower spectral variation in AOD), whereas presence of sub-micron particle yields high value of  $\alpha$  (or higher spectral

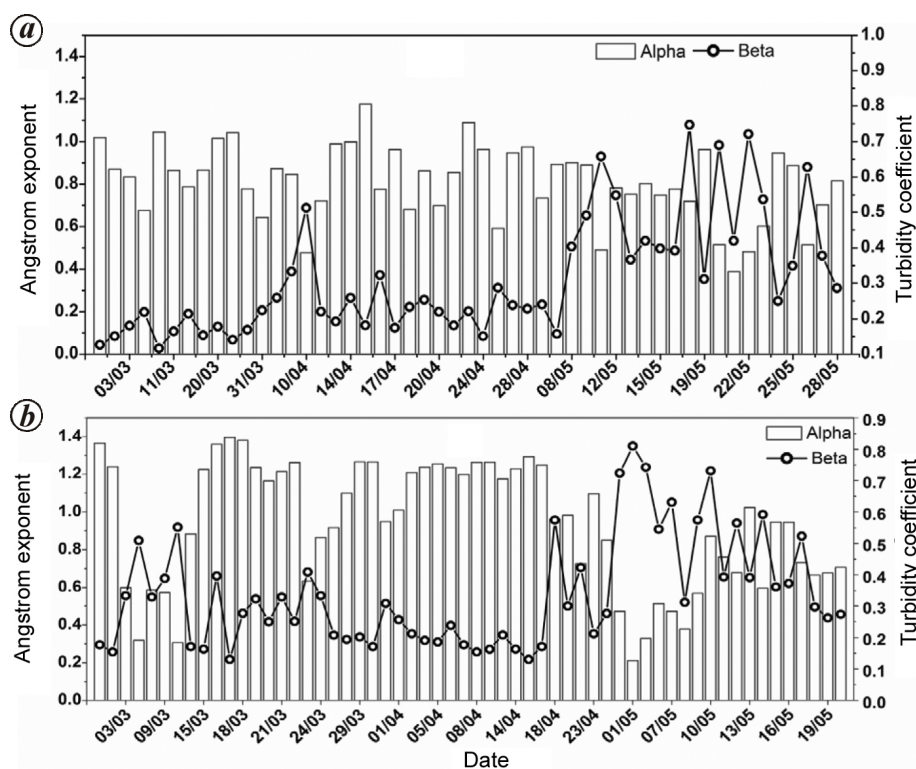


**Figure 6.** Daily variation of Angstrom exponent ( $\alpha$ ) and turbidity coefficient ( $\beta$ ) over (a) DDN and (b) KVT during pre-monsoon seasons.

variation in AOD). Figure 6 shows the daily variation of  $\alpha$  and  $\beta$  over both DDN and KVT. Here, we look into the inter-seasonal variation, which shows no definite variation in  $\alpha$  and  $\beta$ , but slightly decreases in  $\alpha$  and increases in  $\beta$  in May over both the sites. Low values of  $\alpha$  in May indicate a relative dominance of coarse mode particles (dust) over both the sites which are supported by the value of  $\beta$ . The presence of coarse mode aerosol is due to dust transportation from the western region, which has been analysed through back trajectory analysis in Figure 4 along with variation of relative humidity.

The value of  $\alpha$  in May ( $0.65 \pm 0.16$ ) over KVT being lower than its value over DDN ( $0.71 \pm 0.21$ ) might be due to two main reasons; first is the dominance of marine aerosols, e.g. sea-salt over KVT leads to the low value of  $\alpha$  and second is transportation of anthropogenic aerosols from highly polluted cities in northern region of India to the DDN along with coarse mode particles (dust) which are transported from the Arabian countries. The second reason leads to relatively high value of  $\alpha$  over DDN compared to KVT in May, which is supported by variation of spectral AOD shown in Figure 6.

During March and April,  $\alpha$  is observed to be higher over KVT ( $1.04 \pm 0.29$ ) than DDN ( $0.86 \pm 0.19$ ) due to transportation of continental anthropogenic aerosols from the Indian mainland, which is shown in back trajectory analysis (Figure 4).

### Volume size distribution over KVT

Aerosols distribution in vertical column under different conditions is important to understand while studying the types of aerosols. The aerosol volume size distribution ( $dv/d\ln r$ ) has been derived from the spectral Sun and sky radiance data from Nakajima *et al.*<sup>19</sup> over KVT. Over DDN, aerosol volume size distribution has been derived using King's inversion theory from MICROTUPS-II sun-photometer and ozone monitor. Detailed methodology and information have been described in a few studies<sup>27-29</sup>. Figure 7 describes the monthly variation of aerosol volume size distribution over DDN and KVT respectively, during pre-monsoon season. Two distinct types of aerosols have been identified using volume size distribution: coarse (radius  $> 0.6 \mu\text{m}$ ) and fine (radius  $< 0.6 \mu\text{m}$ ). Condensation of gas-phase reaction products leading to the homogenous heteromolecular nucleation, growth of large particles and mixing of two air masses with different aerosol populations<sup>30</sup>, which may be the reason for the tendency of bimodal structure of volume size distribution.

$$dv/d \ln r = \{V/\sigma (2\pi)^{1/2} \exp[-0.5(\ln R/R_v)^2/\sigma^2]\}. \quad (1)$$

Equation (1) describes the log-normal distribution of each mode particles<sup>31</sup>, where  $dv/d \ln r$  is the volume size distribution of aerosol,  $V$  is the columnar volume of particles per

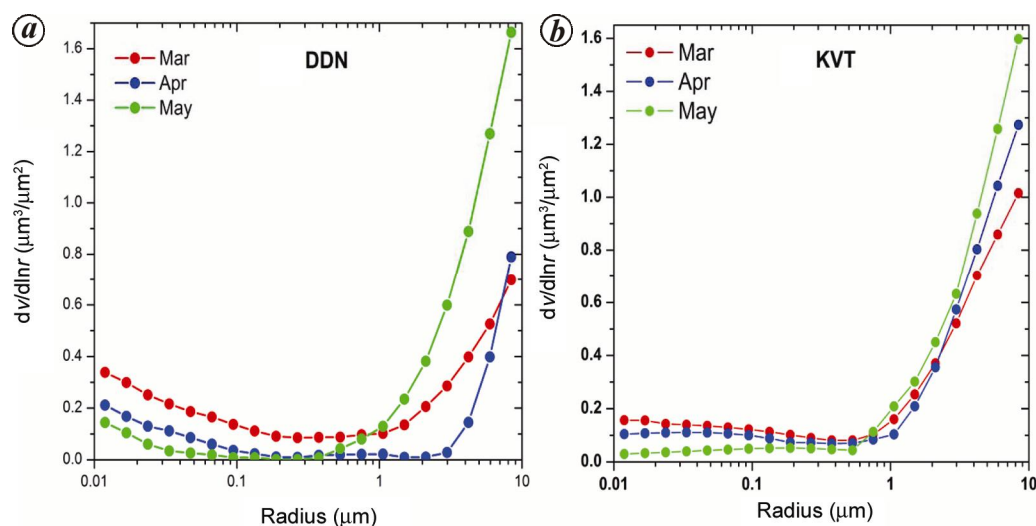


Figure 7. Monthly variation of aerosol volume size distribution over (a) DDN (b) KVT during pre-monsoon.

unit cross-section of atmospheric column,  $R$  is the radius of particle,  $R_v$  is the volume geometric mean radius and  $\sigma$  is the geometric standard deviation.

The volume size distribution for coarse mode is found to be high in May, which suggests the loading of coarse mode aerosols in the atmosphere due to transportation of dust aerosols from western countries (Arabian countries) over DDN. The distribution of fine mode aerosols has decreased gradually from March to May. Concentration of fine mode aerosols is observed to be high with respect to KVT due to transportation of polluted dust from metro cities, for e.g. Delhi as well as vertical transportation of aerosols from valley region to DDN due to diurnal cycle of atmospheric boundary dynamics. Sudden increment in coarse mode aerosols has been detected during May due to dominance of dust aerosols. Table 1 describes the variations of volume size distribution ( $V$ ) and volume geometric mean radius ( $R_v$ ) over both the sites during the study period.

Similar to DDN, volume size distribution for coarse mode aerosols has been observed to be higher in May than March and April. This could be due to the transportation of dust aerosols during May, which has been detected through back trajectories analysis (Figure 4). The all-time value of  $dv/d \ln r$  for coarse mode aerosols is found to be higher over KVT than over DDN. It could be due to the all-time presence of marine aerosols over KVT, which are coarser. A small shift has been observed in the fine mode particles towards coarse mode particles due to hygroscopic growth of fine anthropogenic aerosols over KVT, which is clearly seen in Figure 4. In Figure 4, back trajectories are shown along with relative humidity concentration over both the sites, which is found to be higher over KVT (60–90%) than over DDN (30–60%). There is chance of hygroscopic growth of particles over KVT, which has been detected in volume size distribu-

tion. Decrement in fine mode aerosols has been observed due to the wind pattern which transited from the Indian mainland (north-easterly) to Arabian countries (north-westerly) during March to May, respectively.

#### Single scattering albedo

Scattering optical depth approximated from the aerosol scattering phase function using diffused radiance measured at different angles has been used to compute single scattering albedo (SSA) over KVT using CIMEL sunphotometer<sup>20</sup>. CIMEL sunphotometer provides SSA values in four different wavelengths (440, 670, 870 and 1020 nm); whereas over DDN, SSA has been estimated from BC concentration monitored by an aethalometer using aerosol scattering coefficient and absorbing co-efficient. Detailed equations and methodology are shown in ref. 32. The aerosol absorption coefficient was determined from the data on soot (BC) concentration which are measured through aethalometer using eq. (2) in the given wavelengths (370, 470, 520, 590, 660, 880 and 950 nm)

$$\alpha \text{ (km}^{-1}\text{)} = \alpha_m \text{ (m}^2\text{/g)} \times 10^{-3} \times M_s \text{ (}\mu\text{g/m}^3\text{)}, \quad (2)$$

where  $\alpha$  is the aerosol absorbing coefficient. The value of  $\alpha_m$  is the specific cross-section of absorption = 4.61 m<sup>2</sup>/g (at the wavelength of 0.53  $\mu\text{m}$ ) as per the results of theoretical calculations for dispersed soot particles as well as from literature data<sup>33–35</sup>. Mass concentration of soot ( $M_s$ ) collected using aethalometer and eq. (3) allows us to estimate the single scattering albedo.

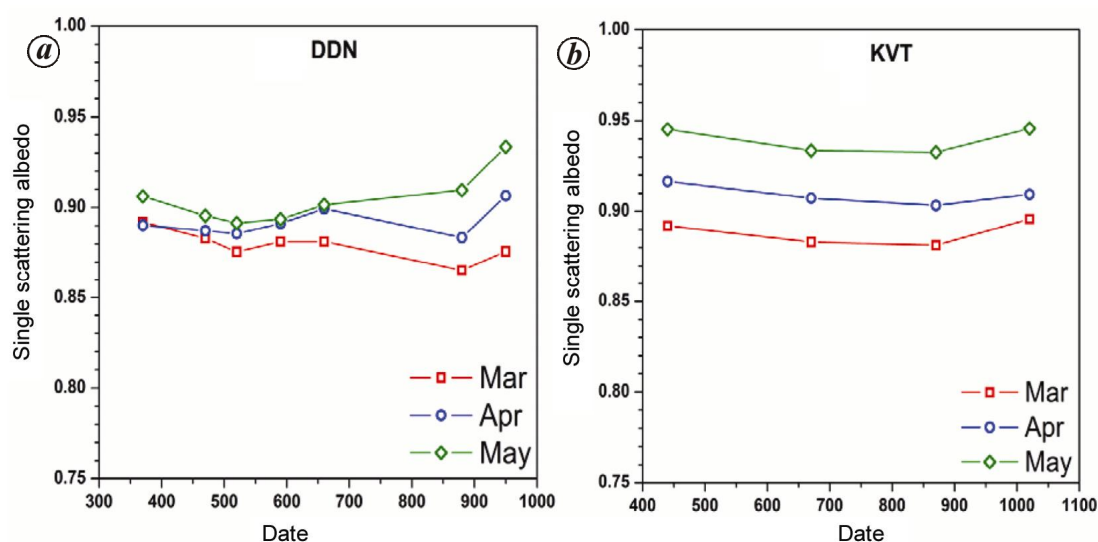
$$\omega = [1 + 0.3x\alpha_m \times P_s x (1-R)^y]^{-1}, \quad (3)$$

where  $P_s = M_s/M_A$  is the relative content of soot in dry particles and  $M_A$  is the concentration of the atmospheric

**Table 1.** Variations of aerosol volume size distribution along with geometric mean radius over DDN and KVT

Month	Type of particle	Parameters	Over DDN (Dehradun)	Over KVT (Kavaratti)
March	Fine mode	$V^*$	0.171	0.121
		$R_v^*$	0.092	0.118
	Coarse mode	$V$	0.306	0.498
		$R_v$	5.047	0.124
April	Fine mode	$V$	0.074	0.094
		$R_v$	0.054	0.161
	Coarse mode	$V$	0.178	0.556
		$R_v$	5.422	4.914
May	Fine mode	$V$	0.038	0.043
		$R_v$	0.080	5.232
	Coarse mode	$V$	0.656	0.688
		$R_v$	6.876	5.179

\* $V$  is the volume concentration ( $\mu\text{m}^3 \mu\text{m}^{-2}$ ) and  $R_v$  ( $\mu\text{m}$ ) is the volume geometric mean radius.

**Figure 8.** Monthly variation of single scattering albedo over (a) DDN (b) KVT during pre-monsoon.

aerosol. The parameter of condensation activity  $\gamma = 0.35$  was collected using literature studies and used for estimating the single scattering albedo  $\omega$ . Atmospheric aerosol has been calculated using eq. (4)

$$M_A (\mu\text{g}/\text{m}^3) = 2 \times \rho (\text{g}/\text{cm}^3) \times 10^2 \times \sigma (\text{km}^{-1}), \quad (4)$$

where  $\rho = 1.8 \text{ g}/\text{cm}^3$  (characteristics of continental aerosol) is the density of the particulate matter. Then, relative content of soot particle has been estimated;  $\sigma$  is the scattering coefficient. Estimation of scattering coefficient is given in ref. 32. Figure 8 describes the comparison of SSA over DDN and KVT at different wavelengths in pre-monsoon season. SSA has been found to be lower ( $<0.88$ ) during March–April over DDN, which increased ( $>0.90$ ) during May. An increase in SSA with decrease in  $\alpha$  value

indicates dominance of concentration of scattering dust particles in the atmosphere during May over DDN.

A rise in SSA was observed during late pre-monsoon (May) over KVT. SSA found to be high in May that depicts the loading of scattering dust particles over KVT, which are transported along with air mass from north-west region (Arabian countries) (Figure 4)<sup>36</sup>. Spectral behaviour of SSA depends on the nature of the aerosol particles<sup>37</sup>. The hygroscopically growth of water-absorbing aerosols in the presence of water vapour contribute the higher SSA at longer wavelength, which is already seen in volume size distribution curves. At longer wavelength, the difference between finer and coarse mode particles is found to be higher than at shorter wavelength indicating the dominance of absorbing aerosols over both the sites during March and April. Table 2 describes the seasonal

**Table 2.** SSA values of the present and other studies over the Indian subcontinent

Stations	References	SSA (pre-monsoon)
Kavaratti, Lakshadweep (10.55°N, 72.62° E)	This study	0.91 ± 0.008
Dehradun, Uttarakhand (30°30'N and 78°36'E)	This study	0.89 ± 0.007
Himalayan region (27.59°N, 85.31°E)	38	0.80
Kanpur (23.43°N, 80.33°E)	11*	0.63 ± 0.06
Bangalore (13°N, 77°E)	39	0.94
Ahmedabad (23.03°N, 72.5°E)	40	0.88 ± 0.03
Delhi (28.63°N, 77.17°E)	41	0.83 ± 0.08

\*Data reported for 2002 at 670 nm.

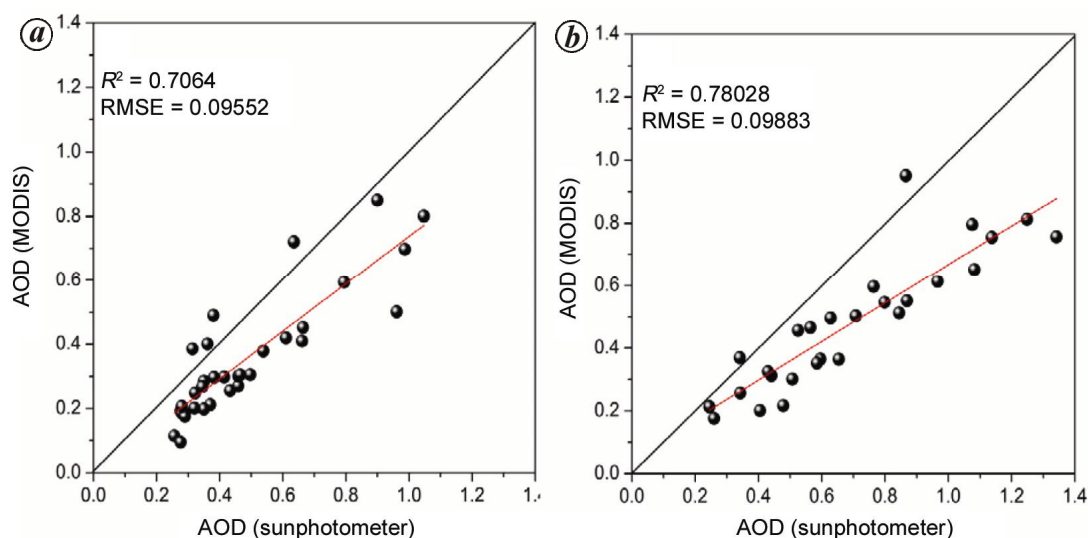


**Figure 9.** Comparison of AOD *in situ* measurements with the MODIS-derived AOD over (a) DDN and (b) KVT.

mean values of SSA found over Kavaratti and summarizes them along with other studies over different locations in the Indian subcontinent. All the studies except Singh *et al.*<sup>11</sup> agree with higher SSA in pre-monsoon season indicating a large mixing of scattering aerosols in the atmosphere.

#### Comparison with MODIS data

AOD datasets which are measured through sunphotometer have been compared with the MODIS-derived AOD over both the continental (DDN) and marine (KVT) observational sites. Figure 9 describes the scatter plots between AOD derived from sunphotometer and MODIS over both sites in India. Good statistical agreement has been observed between MODIS and sunphotometer derived AOD along with  $R^2 = 0.70$  over DDN and  $R^2 = 0.78$  over KVT. The root mean square error (RMSE) is found to be minimal (~0.09) over both sites.

AOD from sunphotometer overestimates the MODIS-derived AOD during this study. The correlation between MODIS and sunphotometer derived AOD is found to be less over continental site than marine site. It may be

because retrieval of AOD over land is more difficult than over ocean.

#### Conclusion

Variation of aerosol optical properties during pre-monsoon season over two different sites, namely, DDN (continental) and KVT (marine) are described in this article. Both the sites have different aerosol optical properties as observed during this study. The main conclusions from this study are summarized as follows:

- Strong seasonal influence has been observed over both the sites during this study. The dust transportations increase the loading of coarse particles over DDN, whereas dust along with marine aerosols lead to increment in coarse particles over KVT during May. In March and April, the influence of anthropogenic aerosols from surrounding polluted cities and from India mainland increases the concentration of finer particles over DDN and KVT respectively. The analysis of seven day back trajectories was supported the facts.
- Spectral variation of AOD suggests that the extra loading of aerosols is due to dust transportation over

DDN during May; whereas over KVT, it is due to the transported continental aerosols from the Indian mainland, which are mostly anthropogenic aerosols. This has been proved with the analysis of Angstrom exponent over both the sites.

- Lower value of  $\alpha$  associated with higher value of  $\beta$  was observed in May over DDN and KVT. These values depict the influences of advected coarse-mode particles, which are also supported by the spectral variation of AOD during the study period.
- Volume size distribution describes bimodal distribution over both the sites. High concentration been found in longer radius due to transportation of dust aerosols in May over both the sites. Concentration of fine mode aerosols is observed to be higher over continental site (DDN) than over marine site (KVT) due to polluted dust. Hygroscopic growth of fine anthropogenic aerosol has been detected over KVT.
- Wavelength-dependent SSA was found during this study. SSA value increases with wavelength during May due to presence of dust aerosols which are scattering in nature; whereas, reverse variation has been observed for the anthropogenic aerosols.
- Comparison of the AOD derived from sunphotometer and MODIS provides good statistical agreement along with high correlation and low RMSE.

1. Forster, P. *et al.*, Changes in atmospheric constituents and in radiative forcing. In *Climate Change 2007: The Physical Science Basis-Contribution of Working Group I to the Fourth Assessment Report of the Intergovernmental Panel on Climate Change* (eds Solomon, S. *et al.*), Cambridge University Press, Cambridge, UK, 2007, pp. 153–171.
2. Ramanathan, V. *et al.*, Indian Ocean Experiment: an integrated analysis of the climate forcing and effects of the great Indo-Asian haze. *J. Geophys. Res.*, 2001, **106**, 28371–28398.
3. Chung, C. E., Ramanathan, V., Kim, D. and Podgorny, I. A., Global anthropogenic aerosol direct forcing derived from satellite and ground-based observations. *J. Geophys. Res.*, 2005, **110**, D24207; doi: 10.1029/2005JD006356.
4. Adhikary, B. *et al.*, Characterization of the seasonal cycle of South Asian aerosols: A regional-scale modelling analysis. *J. Geophys. Res.*, 2007, **112**, D22S22; doi: 10.1029/2006JD008143.
5. Haywood, J. M. and Shine, K. P., Multi-spectral calculation of direct radiative forcing of tropospheric sulphate and soot aerosols using column model. *Q. J. R. Meteorol. Soc.*, 1997, **123**, 1907–1930.
6. Kaufman, Y. J., Tanre, D. and Boucher, O., A satellite view of aerosol in climate system. *Nature*, 2002, **419**, 215–223.
7. Satheesh, S. K. and Ramanathan, V., Large differences in the tropical aerosol radiative forcing at the top of the atmosphere and Earth's surface. *Nature*, 2000, **405**, 60–63.
8. Vinoj, V. and Satheesh, S. K., Measurements of aerosol optical depth over Arabian Ocean during summer monsoon season. *Geophys. Res. Lett.*, 2003, **30**(5), 1263; doi: 10.1029/2003JD0043296.
9. Dey, S., Tripathi, S. N., Singh, R. P. and Holben, B. N., Influence of dust storms on aerosol optical properties over the Indo-Gangetic basin. *J. Geophys. Res.*, 2004, **109**, D20211; doi: 10.1029/2004JD004924.
10. Chinnam, N., Dey, S., Tripathi, S. N. and Sharma, M., Dust events in Kanpur, northern India: Chemical evidence for source and implications to radiative forcing. *Geophys. Res. Lett.*, 2006, **33**, L08803; doi: 10.1029/2005GL025278.
11. Singh, R. P., Dey, S., Tripathi, S. N., Tare, V. and Holben, B. N., Variability of aerosol parameters over Kanpur, northern India. *J. Geophys. Res.*, 2004, **109**, D23206; doi: 10.1029/2004JD004966.
12. Jethva, H., Satheesh, S. K. and Srinivasan, J., Seasonal variability of aerosols over the Indo-Gangetic basin. *J. Geophys. Res.*, 2005, **110**, D21204; doi: 10.1029/2005JD005938.
13. Dey, S., Tripathi, S. N., Singh, R. P. and Holben, B. N., Seasonal variability of the aerosol parameters over Kanpur, an urban site in Indo-Gangetic basin. *Adv. Space Res.*, 2005, **36**, 778–811; doi: 10.1016/j.asr.2005.06.040.
14. Eck, T. F. *et al.*, Climatologically aspects of the optical properties of fine/coarse mode aerosol mixtures. *J. Geophys. Res.*, 2010, **115**, D19205; doi: 10.1029/2010JD014002.
15. Sikka, D. R., Desert climate and its dynamics. *Curr. Sci.*, 1997, **72**, 35–46.
16. Kant, Y., Patel, P., Mishra, A. K., Dumka, U. C. and Dadhwal, V. K., Diurnal and seasonal aerosol optical depth and black carbon in the Shiwalik Hills of the north western Himalayas: A case study of the Doon valley, India. *Int. J. Geol., Earth Environ. Sci.*, 2012, **2**(2), 173–192.
17. Moorthy, K. K. and Satheesh, S. K., Aerosol characteristics over Minicoy: evidence of influence of mineral dust transport. *J. Mar. Atmos. Res.*, 2000, **2**, 25–31.
18. Holben, B. N. *et al.*, AERONET – a federated instrument network and data archive for aerosol characterization. *Remote Sensing Environ.*, 1998, **66**(1), 1–16.
19. Nakajima, T., Tonna, G., Boi, P., Kaufman, Y., and Holben, B., Use of sky brightness measurements from ground for remote sensing of particulate polydispersions. *Applied Optics*, 1996, vol. 35, No. 15, pp. 2672–2686.
20. Olmo, F. J., Quirantes, A., Alcantara, A., Lyamani, H. and Alados-Arboledas, L., Preliminary results of a non-spherical aerosol method for the retrieval of the atmospheric aerosol optical properties. *J. Quant. Spectrosc. Radiative Transfer*, 2006, **100**, 305–314; doi: 10.1016/j.jqsrt.2005.11.047.
21. Kaufman, Y. J. and Tanre, D., Algorithm for remote sensing of tropospheric aerosol from MODIS, Algorithm Theoretical Basis Document, ATBD-MOD-02, NASA Goddard Space Flight Center, 85, 1998.
22. Remer, L. A. *et al.*, The MODIS aerosol algorithm, products and validation. *J. Atmos. Sci. (Spec. Issue)*, 2005, **62**, 947–973.
23. Levy, R. C., Remer, L. A. and Dubovik, O., Global aerosol optical properties and application to moderate resolution imaging spectroradiometer aerosol retrieval over land. *J. Geophys. Res.*, 2007, **112**, D13210; doi: 10.1029/2006JD007815.
24. Gogoi, M. M., Moorthy, K. K., Babu, S. S. and Bhuyan, P. K., Climatology of columnar aerosol properties and the influence of synoptic conditions: first-time results from the northeastern region of India. *J. Geophys. Res.*, 2009, **114**, D08202; doi: 10.1029/2008JD010765.
25. Moorthy, K. K., Babu, S. S. and Satheesh, S. K., Temporal heterogeneity in aerosol characteristics and the resulting radiative impact at a tropical coastal station. Part 1: Microphysical and optical properties. *Ann. Geophys.*, 2007, **25**, 2293–2308.
26. Schuster, G. L., Dubovik, O. and Holben, B. N., Angström exponent and bimodal aerosol size distributions. *J. Geophys. Res.*, 2006, **111**, D07207; doi: 10.1029/2005JD006328.
27. King, M. D., Byrne, D. M., Herman, B. M. and Reagan, J. A., Aerosol size distributions obtained by inversion of spectral optical depth measurements. *J. Atmos. Sci.*, 1978, **35**, 2153–2167.
28. King, M. D., Sensitivity of constrained linear inversions to the selection of the Lagrange multiplier. *J. Atmos. Sci.*, 1982, **39**, 1356–1369.
29. Jorge, H. G. and Ogren, J. A., Sensitivity of retrieved aerosol properties to assumptions in the inversion of spectral optical depths. *J. Atmos. Sci.*, 1996, **53**, 3669–3683.

## RESEARCH ARTICLES

---

30. Hoppel, W. A., Fitzgerald, J. W. and Larson, R. E., Aerosol size distributions in air masses advecting off the east coast of the United States. *J. Geophys. Res.*, 1985, **90**, 2365–2379.
31. Seinfeld, J. H. and Pandis, S. N., *Atmospheric Chemistry and Physics: From Air Pollution to Climate Change*, John Wiley, 1997.
32. Panchenko, M. V., Kozlov, V. S. and Terpugova, S. A., Estimation of the single scattering albedo from the data on the content of submicron aerosol, absorbing substance and the parameter of condensation activity in a local volume. In Proceedings of the Eleventh Atmospheric Radiation Measurement (ARM) Science Team Meeting, Atlanta, Georgia, 19–23 March 2001.
33. Clarke, A. D., Noone, K. J., Heintzenberg, J., Warren, G. S. and Covert, D. S., Aerosol light absorption measurement techniques: analysis and intercomparisons, *Atmos. Environ.*, 1987, **21**, 1455–1465.
34. Gundel, L. A., Dod, R. L., Rosen, H. and Novakov, T., The relationship between optical attenuation and black carbon concentration for ambient and source particles. *Sci. Total Environ.*, 1984, **36**, 197–202.
35. Wolff, G. T., Particulate elemental carbon in the atmosphere. *JAPCA*, 1984, **31**, 935–938.
36. Ackerman, T. P. and Toon, O. B., Absorption of visible radiation in atmosphere containing mixtures of absorbing and non-absorbing particles. *Appl. Opt.*, 1981, **20**, 3661–3668.
37. Smirnov, A. *et al.*, Atmospheric aerosol optical properties in the Persian Gulf. *J. Atmos. Sci.*, 2002, **59**, 620–634.
38. Ramana, M. V., Ramanathan, V., Podgorny, I. A., Pradhan, B. B. and Shrestha, B., The direct observations of large aerosol radiative forcing in the Himalayan region. *Geophys. Res. Lett.*, 2004, **31**, L05111; doi: 10.1029/2003GL018824.
39. Babu, S. S., Satheesh, S. K. and Moorthy, K. K., Aerosol radiative forcing due to enhanced black carbon at an urban site in India. *Geophys. Res. Lett.*, 2002, **29**, 1880; doi: 10.1029/2002GL015826.
40. Ramachandran, S. and Kedia, S., Black carbon aerosols over an urban region: radiative forcing and climate impact. *J. Geophys. Res.*, 2010, **115**, D10202; doi: 10.1029/2009JD013560.
41. Soni, K., Singh, S., Bano, T., Tanwar, R. S., Nath, S. and Arya, B. C., Variations in single scattering albedo and Ångström absorption exponent during different seasons at Delhi, India. *Atmos. Environ.*, 2010, **44**, 4355–4363.
42. Chylek, P. *et al.*, Aerosol indirect effect over the Indian Ocean. *Geophys. Res. Lett.*, 2006, **33**, L06806.
43. Eck, T. F., Holben, B. N., Reid, J. S., Dubovik, O., Smirnov, A., O'Neill, N. T., Slutsker, I. and Kinne, S., Wavelength dependence of the optical depth of biomass burning, urban, and desert dust aerosols. *J. Geophys. Res.*, 1999, **104**, 31333–31349; doi: 10.1029/1999JD900923.

ACKNOWLEDGEMENTS. We acknowledge the encouragement received from Director, SAC for carrying out the present study. Valuable suggestions received from Deputy Director, EPSA and Group Director, MPSG are also gratefully acknowledged. We thank the team at ISRO CAL-VAL site in Kavaratti for collecting data on aerosols. We also thank IIRS, Dehradun for providing a chance to collect data.

Received 28 June 2014; revised accepted 7 October 2014

---